Phenotypic delay: mechanistic models and their implications for the evolution of resistance to antibiotics

Martín Carballo-Pacheco[1*], Michael D. Nicholson[1*], Elin E. Lilja[1], Rosalind J. Allen[1,2], and Bartlomiej Waclaw[1,2]

[1]School of Physics and Astronomy, The University of Edinburgh, Peter Guthrie Tait Road, Edinburgh, EH9 3FD, United Kingdom
[2]Centre for Synthetic and Systems Biology, The University of Edinburgh, Edinburgh EH9 3FD, United Kingdom

Abstract

Phenotypic delay – the time delay between genetic mutation and expression of the corresponding phenotype – is generally neglected in evolutionary models, yet recent work suggests that it may be more common than previously assumed. Here, we use computer simulations and theory to investigate the significance of phenotypic delay for the evolution of bacterial resistance to antibiotics. We consider three mechanisms which could potentially cause phenotypic delay: effective polyploidy, dilution of antibiotic-sensitive molecules and accumulation of resistance-enhancing molecules. We find that the accumulation of resistant molecules is relevant only within a narrow parameter range, but both the dilution of sensitive molecules and effective polyploidy can cause phenotypic delay over a wide range of parameters. We further investigate whether these mechanisms could affect population survival under drug treatment and thereby explain observed discrepancies in mutation rates estimated by Luria-Delbrück fluctuation tests. While the effective polyploidy mechanism does not affect population survival, the dilution of sensitive molecules leads both to decreased probability of survival under drug treatment and underestimation of mutation rates in fluctuation tests. The dilution mechanism also changes the shape of the Luria-Delbrück distribution of mutant numbers, and we show this modified distribution provides an improved explanation of previously published experimental data.

1 Introduction

The emergence of resistance to drugs is a significant problem in the treatment of diseases such as cancer [1], and viral [2] and bacterial infections [3]. In the case of infectious diseases, treatment failure can often be attributed to the infecting organism being resistant [4]. However, resistance can also be caused by new genetic mutations in infections with sufficiently high pathogen load [5]. Such *de novo* resistance has been observed in infections caused by *Staphylococcus aureus* during endocarditis [6, 7], *Burkholderia dolosa* [8, 5] and *Pseudomonas aeruginosa* [9, 10] during cystic fibrosis, *Escherichia coli* during asymptomatic bacteriuria [11], and *Helicobacter pylori* [12, 13].

The emergence and spreading of resistant variants in populations of pathogenic cells has received much experimental [14, 15, 16, 17, 18] and theoretical attention [19, 20, 21, 22]. However, most mathematical models assume that a genetic mutation immediately transforms a sensitive cell into a resistant cell [23, 24, 25, 26, 27, 28]. In reality, a new allele (genetic variant) must be expressed to a sufficient level before the cell becomes phenotypically resistant. The time between the occurrence of a genetic mutation and its phenotypic expression is called *phenotypic delay* and is also referred to as delayed phenotypic expression, phenotypic lag, cytoplasmic lag or phenomic lag.

---

* These authors contributed equally

Phenotypic delay was first observed in 1934 by Sonnenborn and Lynch [29] when studying the effect of conjugation on the fission rate of *Paramecium aurelia*. It was observed that, even though the fission rate is determined genetically, the new hybrids initially assumed the fission rates of the parent with whom they shared their cytoplasm, and the new genotype manifested phenotypically only after a few generations. Phenotypic delays were studied during the 1940s and 1950s, both theoretically [30] and experimentally [31, 32]. Interestingly, in their hallmark work on the randomness of mutations in bacteria [33], Luria and Delbrück discussed the possible effect of a phenotypic delay on the estimation of mutation rates. The interest in phenotypic delays waned for the next fifty years, mostly because experimental data failed to reveal their presence [34, 33]. However, Sun et al. [35] recently demonstrated the existence of a phenotypic delay of 3-4 generations in the evolution of resistance of *Escherichia coli* to antibiotics rifampicin, nalidixic acid and streptomycin. Sun et al. attributed this delay to effective polyploidy (see below) and argued that not accounting for a phenotypic delay can cause an underestimation of the mutation rate in fluctuation tests [33, 36].

Here, we generalize these observations and investigate other reasons that may lead to phenotypic delay. We consider three mechanisms: (i) effective polyploidy as in [35], (ii) the dilution of sensitive molecules targeted by the drug, and (iii) the accumulation of resistance-enhancing molecules.

Effective polyploidy refers to the fact that a single cell can contain multiple copies of a given gene. This can be due to gene duplication events or carriage of multicopy plasmids; it also occurs in fast-growing bacteria, which initiate new rounds of DNA replication before the previous round has finished, allowing for a shorter generation time than the time needed to replicate the chromosome [37, 38, 39]. Since a *de novo* resistance mutation happens in only one of the multiple gene copies, it may take several generations before a cell emerges in which all gene copies contain the mutated allele. Until then, sensitive and resistant variants of the target protein coexist in the cell. A phenotypic delay occurs when the resistance mutation is recessive, i.e., the sensitive variant must be replaced by the resistant variant for the cell to become resistant. This is the case for antibiotics which form toxic adducts with their targets [40, 41]. Examples are quinolones that lock the enzyme DNA gyrase onto the DNA and prevent DNA replication [42], and polymixins that bind to lipids in the outer membrane which causes membrane perforation [43, 44].

The *dilution mechanism* also assumes the mutation to be recessive, but in contrast to the polyploidy mechanism it focuses on the removal of the sensitive target protein through the process of cell growth and division. As a mutated cell grows, resistant version of the protein accumulates; a subsequent division creates two cells in which the fraction of the sensitive variant is less than in the parent cell. A single copy of the gene may therefore still cause a considerable delay if the number of sensitive proteins to dilute out is large before resistance can be established.

The *accumulation mechanism* posits that sufficiently many resistant variants of the protein must be produced to cause resistance. This applies to mutations that enhance the expression of drug efflux pumps [45], β-lactamase enzymes that hydrolyze β-lactam antibiotics [46, 47], or mutations that protect ribosomes from tetracycline [48] which restores the active ribosome pool [49]. In these cases, a phenotypic delay could emerge due to the time required for the resistance-enhancing molecule to accumulate in the cell to a level high enough to cause resistance.

We first analyse the three mechanisms using computer simulations and analytic calculations. We find that the accumulation of resistant-enhancing molecules only leads to phenotypic delay within a limited parameter range, while effective polyploidy and the dilution of sensitive molecules lead to phenotypic delay for a broad range of parameters. We then show that while the effective polyploidy mechanism does not affect the probability that a population survives antibiotic challenge, dilution of sensitive protein leads to decreased probability of survival under drug treatment.

We then investigate the possibility of detecting a phenotypic delay experimentally. We first show that the dilution mechanism would cause an underestimation of mutation rates in fluctuation tests compared to the true genetic rate of mutations. In a fluctuation test, one measures the distribution of mutant numbers in replicate populations that have been allowed to grow and evolve for a fixed number of generations. The mutation rate is then estimated by fitting a population dynamics model to the experimental distribution [33, 50]. In agreement with our prediction, the mutation rate of *Escherichia coli* obtained in fluctuation tests has been found to be an order of magnitude smaller than the rate obtained by DNA sequencing [51].

We also show that the dilution mechanism subtly alters the shape of the Luria-Delbrück distri-

bution of mutant numbers. Discrepancies between the shapes of the experimental and theoretically predicted mutant number distributions have been observed since the original experiments of Luria and Delbrück [33, 34, 30, 52], but have never been satisfactorily explained. Using the experimental data set from Boe et al. [52] for fluoroquinolone antibiotics, we show that a mathematical model that includes the dilution mechanism fits the data better than the no-delay Luria-Delbrück model, thus providing indirect evidence for the existence of this type of phenotypic delay in *de novo* evolution of resistance to fluoroquinolones.

2 Results

2.1 Modeling the emergence of phenotypic delay

To explore the characteristic features of the three different phenotypic delay mechanisms – dilution of sensitive molecules, effective polyploidy, and accumulation of the resistant variant – we first simulate an idealised mutagenesis experiment (figure 1a). A population of sensitive bacteria is exposed to a mutagen (e.g., UV radiation [53, 54]) which instantaneously induces mutations in a small fraction of the cells [55, 56], thus providing a well-defined reference point from which we count time. Cells immediately begin to express the mutated allele, but because of the existence of phenotypic delay, they remain sensitive to the antibiotic for some time; phenotypically resistant cells emerge only after a few generations.

We shall investigate the emergence of resistance in two different ways. The first way is to follow a random lineage, starting from a single mutant bacterium (i.e., at each division we follow one of the randomly selected daughter cells) and we measure the waiting time before a phenotypically resistant cell emerges *in that lineage* (SI figure S1). The second way is to track the entire population post mutagenesis, and examine the waiting time before the first phenotypically resistant cell emerges *in the whole population* (figure 1).

Dilution of antibiotic-sensitive molecules: If the resistance mutation is recessive, such that a small number of sensitive target molecules are enough to cause antibiotic sensitivity, a phenotypic delay can arise from the time taken to replace sensitive target molecules by resistant ones. To model this, we assume that each cell has a fixed number n of target molecules, that can be either sensitive or resistant. Initially, all n molecules are sensitive but once a mutation has happened, the cell starts to produce resistant molecules. We suppose that, upon cell division, the n molecules are partitioned stochastically without bias between the two daughter cells, and new molecules are produced to bring the total back to n per cell (figure 1b). For simplicity, cells are considered phenotypically resistant only when they contain no sensitive molecules.

For this mechanism, the length of the phenotypic delay increases approximately logarithmically with the number n of sensitive molecules that need to be diluted for resistance to emerge (figure 1c). To understand this, suppose momentarily that n is a power of 2 and stochasticity can be neglected so that each daughter cell receives exactly half the number of molecules of the parent cell. Then for any lineage stemming from a genotypically mutant cell, the number of inherited sensitive molcules will be 2^{n-1}, 2^{n-2}, ..., as the generations progress. After $\log_2 n$ generations all cells will have a single sensitive molecule and hence the first phenotypically resistant cell will then emerge after $1 + \log_2 n$ generations. In this deterministic setting this will also be the time for the population to become resistant.

In the more realistic case of stochastic segregation of molecules, the probability of resistance along a random lineage after g generations is approximately $\exp(-n2^{-g})$ (see SI Section 1.1). Hence the probability of resistance emerging in a lineage is negligible until generation g set by $2^g \approx n$, when the probability rapidly rises to 1. Therefore, in line with our deterministic reasoning, resistance along a random lineage will emerge after $g \approx \log_2 n$ generations. Interestingly, however, we obtain a different result for the probability that the population produces at least one resistant cell. If we start from x genotypically mutant cells in the population, the first phenotypically resistant cell in the population emerges, on average, after an approximate time $1 + \log_2(n/\log(xn))$ (SI Section 1.1). We can also calculate the resistance probability through a recursion relation (SI Section 1.1); the results fully reproduce the simulation (figure 1c.). The emergence of resistance at the population level is thus accelerated compared to what one would obtain based on deterministic dilution. An extended model in which molecules are distributed in a biased way between the two
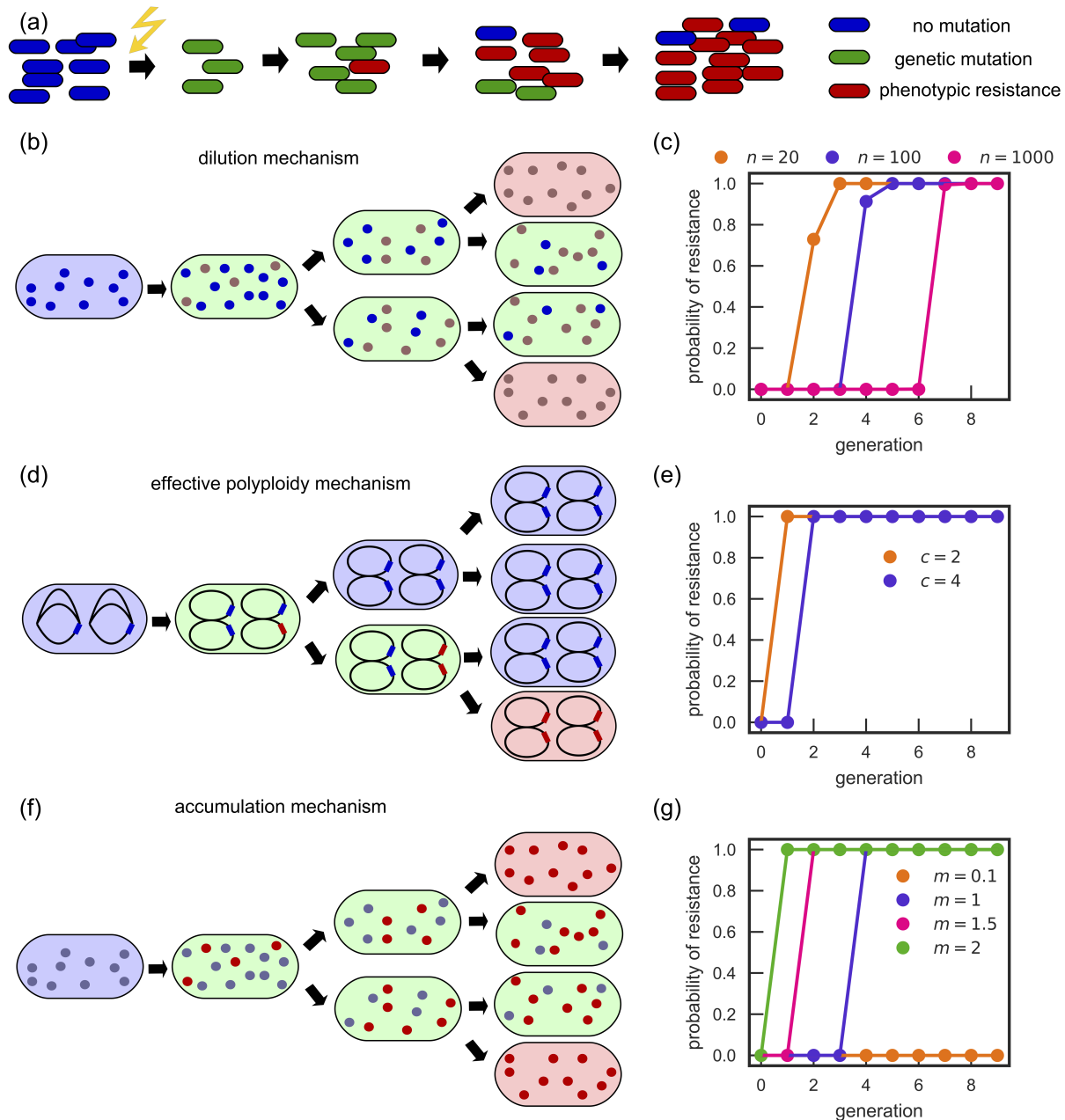
Figure 1: **Models of phenotypic delay.** (a) Schematic representation of a simulated experiment, in which a mutagen (e.g., UV radiation) induces resistant mutations at a particular moment in time. Mutated cells remain sensitive to the antibiotic until after a few generations (phenotypic delay). (b) The dilution mechanism: blue/brown dots denote sensitive/resistant variants of the target molecule. Cells are initially sensitive (green) and become resistant (red) when all sensitive molecules are diluted out. (c) Probability that at least one cell in an exponentially growing population starting with 100 newly genetically mutated cells is phenotypically resistant (dilution model) as a function of the number of generations since the genetic mutation (dots: simulation; lines: theory). Phenotypic delay increases with the number of molecules n to be diluted. (d) The effective polyploidy mechanism: chromosomes are represented as black ellipses, with a sensitive/resistant allele marked blue/red. (e) Same as in (c) but for the effective polyploidy mechanism. Phenotypic delay increases with ploidy c. (f) The accumulation mechanism: blue/red dots denote sensitive/resistant mutants of the resistant-enhancing molecule. Cells become resistant (red) when the cell contains enough resistant molecules. (g) Same as in (c) but for the accumulation model. Phenotypic delay decreases with increasing ratio m of the number of molecules produced during cell cycle and the number of molecules required for resistance.

4

daughter cells, inspired by recent evidence on accumulation of membrane proteins in the daughter cell with the older pole [57, 58, 59, 60], leads to a similar result (SI Section 3). However, the bias decreases slightly the phenotypic delay at a population level (SI figure S3). This is because the bias creates lineages which will be low in the number of resistant molecules.

Effective polyploidy: Rapidly dividing bacteria can become effectively polyploid when they initiate a round of DNA replication before the previous round has finished; this leads to the presence of multiple copies of at least some parts of the chromosome [37] (figure 1d). Crucially, the degree of polyploidy (number of gene copies) depends on the bacterial growth rate, as well as on other factors such as the genetic locus. To model phenotypic delay caused by effective polyploidy, we assume that each cell has a given number c of chromosome copies that is growth-rate dependent according to the well-established Cooper-Helmstetter model of *E.coli* chromosome replication [37] (Methods). Each chromosome copy contains a single allele, encoding the antibiotic target, that can be either sensitive or resistant. Initially all chromosomes have the sensitive allele but a mutation changes one allele from sensitive to resistant. We then simulate the process of DNA replication and cell division, taking account of the fact that duplicated resistant alleles are co-inherited – for example, if a cell has two chromosome copies, one with a resistant allele and the other with a sensitive allele, then upon replication and division, one daughter cell will have two sensitive alleles and the other daughter cell will have two resistant alleles [38] (Methods). We assume that a cell becomes phenotypically resistant when none of its chromosomes contain the sensitive allele (i.e., the resistant allele is assumed to be recessive). In this model, the waiting time until a cell acquires a full suite of resistant chromosomes, i.e. the phenotypic delay, is $\log_2 c$ generations (figure 1e). This delay time is the same whether we track a given lineage or the entire population (since it is deterministic). However, resistance will not occur in all lineages; of the c lineages descended from the original mutant cell, resistance will eventually occur in only one of them [35] (SI figure S1).

We note that effective polyploidy genrally causes a shorter delay than dilution of sensitive molecules: 2 to 3 generations for rapidly growing bacteria ($c = 4$ or 8 [37, 35]), versus 5 generations for the dilution mechanism (assuming $n \approx 500$ typical for the gyrase enzyme targeted by fluoroquinolones [61, 62]). Transition in the probability of resistance is also sharper than for the dilution mechanism in which stochasticity of the segregation process smoothens out the transition (compare figures 1a and e). Finally, for effective polyploidy, we expect only one in every c lineages to become resistant, while for dilution of sensitive molecules, effectively all lineages will eventually become resistant.

Accumulation of resistance-enhancing molecules: Phenotypic delay can also emerge due to the time needed to accumulate resistance-enhancing molecules to a sufficiently high level (figure 1f). To model this mechanism, we suppose that during each cell cycle a genotypically resistant cell produces M_p resistance-enhancing molecules, which are randomly distributed between daughter cells at division. A cell becomes resistant when it has M_r or more resistance-enhancing molecules. Interestingly, considering either a single lineage (SI figure S1) or the entire population (figure 1g), we find that phenotypic delay emerges only within a limited parameter range: $1 \lesssim m \lesssim 2$, where $m = \frac{M_p}{M_r}$ is the ratio of the number of molecules produced during a cell cycle and the number of molecules needed for resistance. The origin of this limited parameter range is most easily explained by considering a single lineage. Tracking a lineage arising from a single mutant cell, the cell in the gth generation will be born with an average of $M_p(1 - 2^{-g})$ molecules (SI Section 1.2). The steady-state number of molecules (found by taking $g \to \infty$) is M_p. Thus if $m < 1$, the steady state number of molecules will be always smaller than the minimum required number M_r, and the lineage will never become phenotypically resistant. Conversely, if $m > 1$, phenotypic resistance will emerge after approximately $\tau = -\log_2(1 - 1/m)$ generations when the average number of resistance-enhancing molecules exceeds M_r. But for the delay to be detectable – at least one generation ($\tau \geq 1$) – we require $m \leq 2$. Considering now the scenario where we track the entire population, we again expect the steady-state molecule number M_p to be rapidly reached for all cells, so that there will be no phenotypic resistance for $m < 1$. Further, if resistance does emerge (for $m > 1$), it will do so more quickly in the entire population than along the random lineage (as resistance may be acquired in any lineage). We thus expect an even tighter upper bound on the value of m for phenotypic delay to manifest itself on the population level.

Since our analysis shows that, for this mechanism, phenotypic delay only emerges in a narrow parameter range, we conclude that the accumulation of resistance-enhancing molecules is unlikely

5

to be biologically relevant in causing phenotypic delay. Therefore we do not explore this mechanism further.

2.2   Combining effective polyploidy and dilution

In reality, for a recessive resistance mutation, we expect both the effective polyploidy and dilution mechanisms to contribute to the phenotypic delay. To see this, we simulated a model combining the two mechanisms, tracking the emergence of resistance at a single-cell and population level. Our simulations predict a phenotypic delay with characteristics of both mechanisms (figure 2).

Focusing first on a single lineage (figure 2a,b), we observe that the long-term probability of phenotypic resistance depends on the ploidy c, tending approximately to $1/c$, as expected for the effective polyploidy mechanism, while the approach to this value is gradual as expected for the dilution mechanism. Combining both mechanisms increases the length of the delay compared to either mechanism acting in isolation. Following Sun et al. [35], we also calculate the phenotypic penetrance defined as the proportion of genetic mutants which are phenotypically resistant, in the entire population. The expected phenotypic penetrance is (see SI for derivation Section 1.3):

$$\begin{cases} 0 & 0 \le g < \log_2 c, \\ (1 - 2^{-g})^n \prod_{i=0}^{\log_2 c - 1}(1 - 2^{-(g-i)})^{n(1-2^i/c)} & \log_2 c \le g. \end{cases} \tag{1}$$

Note that $n = 0$ corresponds to only the effective polyploidy mechanism, while $c = 1$ corresponds to only the dilution mechanism being present. The piecewise form of Eq. (1) arises because no cell can become phenotypically resistant until all its chromosomes have the resistant allele. Figure 2d shows that the phenotypic penetrance predicted by Eq. (1) increases gradually with time (characteristic of the dilution mechanism) but with a delay determined by effective polyploidy.

We now return to computer simulations to study the emergence of resistance on the population level following mutagenesis (figure 1). In general, both the ploidy c and the number of antibiotic target molecules per cell n will depend on the doubling time t_d (or growth rate) of cells. To be more specific, we consider resistance of *E. coli* to fluoroquinolone antibiotics that arises through mutations in the DNA gyrase (protein targeted by the antibiotic). Gyrase abundance as a fraction of the proteome has been found to be independent of the growth rate [63]. We therefore assume that the number n of gyrases per cell is proportional to the cell volume V. We model the volume as $V \propto 2^{\lambda/\lambda_0}$, where $\lambda = (\ln 2)/t_d$ is the growth rate and $\lambda_0 = 1\text{h}^{-1}$ [64, 65, 66, 67], and polyploidy using the Cooper-Helmstetter model [37] (see Methods and Model for details). We find for slow-growing cells ($t_d = 60\,\text{min}$) that $c = 2$ and $n = 20$, while for fast-growing cells ($t_d = 30\,\text{min}$), $c = 4$ and $n = 40$. Note that here we do not assume realistic values of n because the minimum number n_r of poisoned sensitive gyrase molecules required to inhibit growth is probably much higher than $n_r = 1$ assumed in the model. n should be therefore interpreted more correctly as the number of "units" of gyrase, with one unit equivalent to n_r molecules. Figure 2c shows that the phenotypic delay is longer for the fast-growing population, and that this is mostly caused by the increase in the number of molecules n (SI figure S4). We also observe that protein dilution leads to a smoother transition between sensitivity and resistance than the transition due to effective polyploidy alone.

2.3   Dilution mechanism, but not effective polyploidy, affects the probability of clearing an infection

To understand better the practical significance of phenotypic delay, we simulated antibiotic treatment of an idealised bacterial infection (figure 3). We assume that, before treatment, the population of bacteria grows exponentially in discrete generations, and cells mutate with probability $\mu = 10^{-7}$ per cell per replication. When the population size reaches 10^7, an antibiotic is introduced; this causes all phenotypically sensitive bacteria to die, leaving only phenotypically resistant cells (figure 3b). We are interested in the probability that the bacterial infection survives the antibiotic treatment, a concept closely related to evolutionary rescue probability, i.e., the probability that cells can survive a sudden environmental change thanks to an adaptive mutation [68, 35, 69]. Since sensitive cells do not reproduce in our simulations in the presence of the antibiotic, survival can only be due to pre-existing mutations (standing genetic variation).
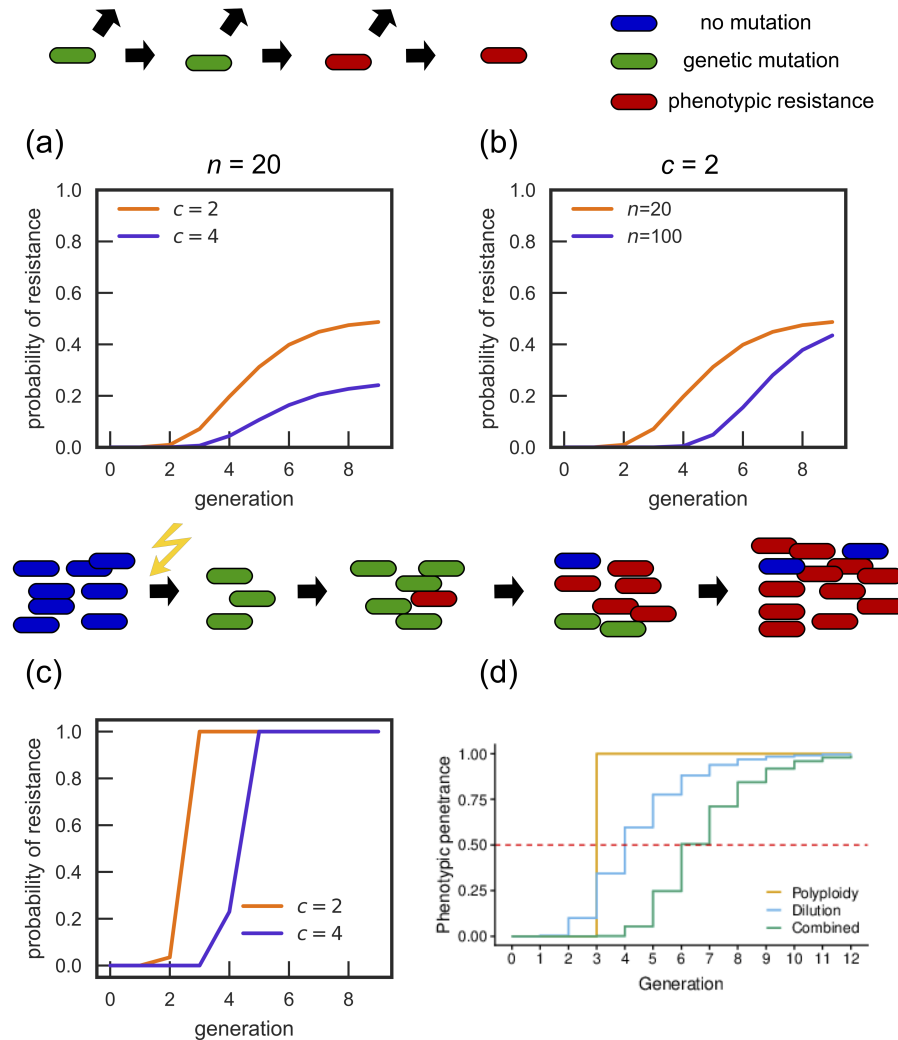
Figure 2: **Joint effect of the dilution and effective polyploidy mechanisms.** (a-b) Probability of resistance of a single mutated cell. While the long-term probability is defined by the effective polyploidy, short-term behaviour is determined by the dilution mechanism, leading to longer phenotypic delays than the effective polyploidy mechanism would do. (c) Population-level probability of resistance versus the number of generations from the mutation event, for $n = 20$. The combined mechanism leads to smoother curves than the effective polyploidy mechanism and longer delays than for both mechanism individually. (d) Phenotypic penetrance (ratio of phenotypically resistant to genotypically resistant cells, obtained from Eq. (1)) for the different mechanisms, for $c = 8, n = 8$. The dashed red line indicates when the phenotypic penetrance surpasses $1/2$, which is the threshold used by Sun et al. [35] to define the emergence of phenotypic resistance. With this definition, the dilution mechanism plus effective polyploidy doubles the delay (generation 6 as opposed to generation 3).
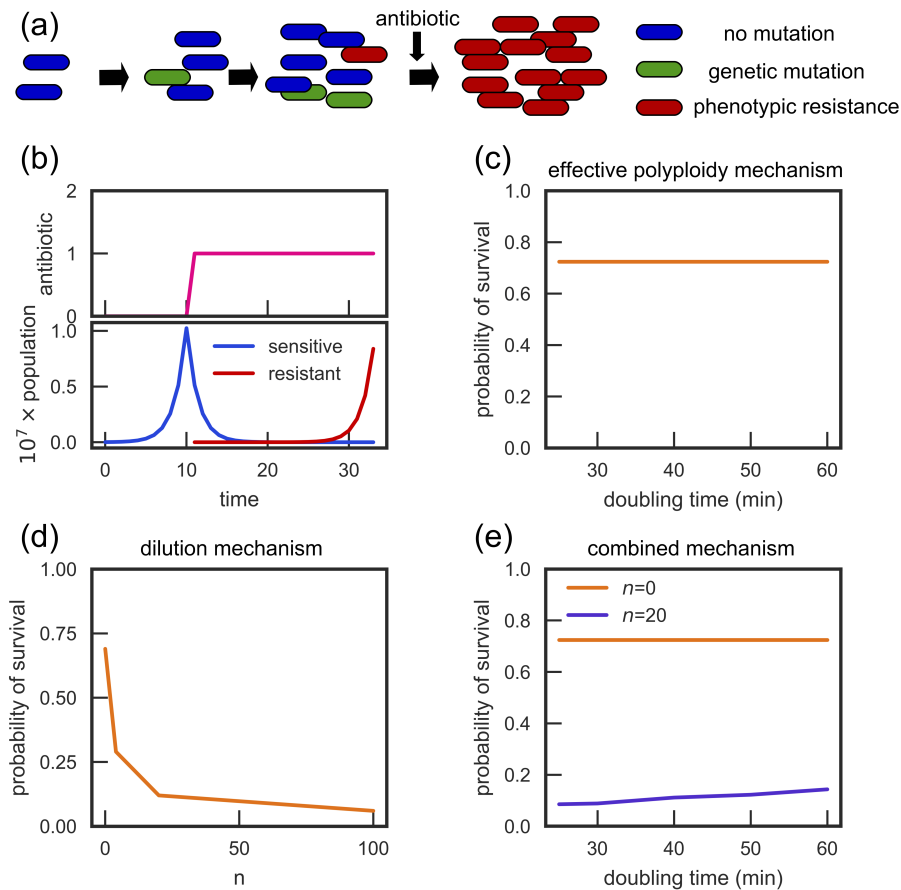
7

Figure 3: **Phenotypic delay decreases the probability of a bacterial infection surviving antibiotic treatment** (a-b) A schematic of the simulated infection: a population of exponentially replicating sensitive cells is exposed to an antibiotic when the population reaches 10^7 cells. Only phenotypically resistant cells survive the antibiotic. Time and antibiotic concentration in panel (b) have arbitrary units. (c) The probability of survival for the effective polyploidy mechanism is independent of the doubling time (and hence the ploidy). (d) For the dilution mechanism, the probability of survival decreases with the number of molecules n which need to be diluted out before the cell becomes phenotypically resistant. (e) In a combined dilution-and-effective polyploidy model, the survival probability increases with the doubling time.
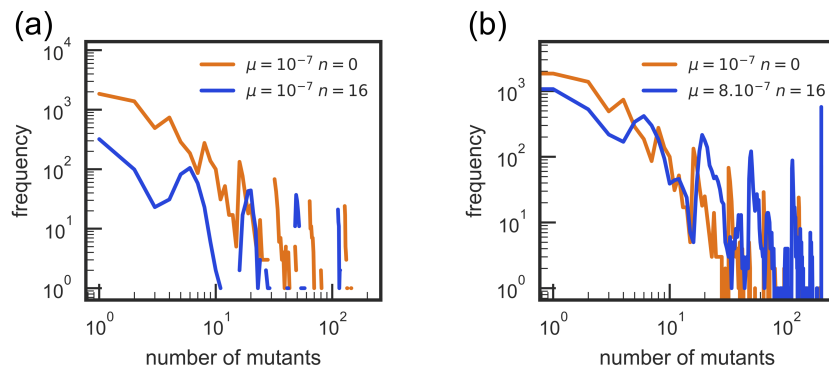
Figure 4: **The dilution model affects the probability distribution of the number of resistant cells.** The frequency of mutants for a simulated fluctuation test with 10,000 samples, for the model with $n = 0$ (no delay) and $n = 16$. (a) Distributions for both models for a fixed $\mu = 10^{-7}$. (b) Distributions for the case when μ in the dilution model has been adjusted to minimize the difference to the no-delay model (values in the inset).

We first consider the effective polyploidy model, with ploidy c controlled by the doubling time t_d. In agreement with Sun et al. [35], we find that t_d has no effect on the survival probability (figure 3c). This is due to a cancellation of two effects: the increased number of gene copies increases the per-cell chance of genetic mutation, but also increases the length of the phenotypic delay. In contrast, phenotypic delay caused by the dilution of sensitive molecules does affect the survival probability (figure 3d). The survival probability strongly depends on n, and decreases significantly from 0.69 for $n = 0$ to 0.06 for $n = 100$.

We also simulated a mixed case where both the effective polyploidy and dilution mechanisms combined, with ploidy c and molecule number n determined by the doubling time t_d as described in Sec. 2.2. In this case the survival probability does depend on the doubling time (figure 3e; blue line). This is mostly caused by the change in the molecular number n as a function of doubling time. If we neglect the dependence of n on t_d, the effect is much smaller, although there is still some dependence on t_d because the rate of resistant protein production depends on the resistant gene copy number, which increases en route to the full suite of resistant chromosomes (SI figure S4).

2.4 Phenotypic delay due to dilution changes the Luria-Delbrück distribution and biases mutation rate estimates

The scenario discussed in the previous section is equivalent to the Luria-Delbrück fluctuation test [33, 70], which has been extensively studied theoretically [71, 72, 73, 50, 74, 75, 76, 77, 78]. A small number of sensitive bacteria are allowed to grow until the population reaches a certain size. The cells are then plated on a selective medium (often an antibiotic) to reveal the number of mutated bacteria in the population. The distribution of the number of mutants (measured over replicate experiments) is termed the Luria-Delbrück distribution. This distribution has a power-law tail caused by mutational "jackpot" events [33, 70, 77] in which rare, early-occurring mutants produce many descendants in the population. The fluctuation test and the corresponding mathematical model have been used to estimate mutation rates in bacteria. Here, we discuss the effect of phenotypic delay on the Luria-Delbrück distribution and on the resulting mutation rate estimate.

First, we note that phenotypic delay caused by effective polyploidy alone does not affect the Luria-Delbrück distribution. As discussed in the previous section, this is due to an exact cancellation of two effects: increased ploidy leads to more mutations per bacterium but also a longer phenotypic delay [35]. In contrast, the dilution model does alter the Luria-Delbrück distribution. Figure 4a shows that, for a fixed mutation probability μ and initial and final population sizes, phenotypic delay due to dilution causes an increase in the number of replicate experiments yielding zero resistant mutants, and a decrease in the number of experiments yielding intermediate numbers of resistant mutants. The number of experiments yielding very large numbers of mutants (>200),

9

due to jackpot events, is unaffected by the delay – this is because mutants that arise early will have had sufficient time to dilute out all sensitive molecules before being exposed to the antibiotic.

From a practical point of view, the mutation probability is often unknown and the fluctuation test is used to estimate it. To investigate the effect of phenotypic delay on the measured mutation probability, we simulated the fluctuation test for the dilution model with $n = 16$, for a range of mutation probabilities. We compared the resulting mutant number distributions to that obtained in an equivalent simulation without phenotypic delay, with mutation probability $\mu = 10^{-7}$. Using a genetic algorithm [79] to minimize the L_2 norm between the distributions with and without phenotypic delay, we found that the phenotypic delay model required a much larger mutation probability ($\mu = 8 \times 10^{-7}$) to reproduce the distribution of the no-delay model. This suggests that neglecting phenotypic delay when fitting theory to fluctuation test data could significantly underestimate the true mutation probability. We also note that the "closest match" distributions with and without phenotypic delay are not exactly identical (figure 4b). The model with phenotypic delay leads to a larger number of jackpot events (as might be expected since the mutation probability is higher) and a reduced number of replicates with few mutants, consistent with suppression of late-occuring mutants by the phenotypic delay.

Our result explains the apparent discrepancy between mutations probabilities estimated through different methods. Lee et al. measured the mutation probability of *E. coli* using both fluctuation tests (fluoroquinolone nalidixic acid as selective agent) and whole-genome sequencing [51]. The fluctuation test underestimated the mutation probability by a factor of 9.5; Lee et al. suggested that this could be caused by phenotypic delay [51]. To see whether our dilution model could explain this, we simulated the 40-replicate, 20 generation fluctuation test experiment of Lee et al. [51], using the mutation probability as estimated by whole-genome sequencing ($\mu = 3.98 \times 10^{-9}$, total for all mutations givins sufficient resistance to nalidixic acid), for differing values of the number n of target "units" (gyrase molecules). For each n we simulated 1000 realisations of the 40-replicate experiment, and for each realisation we estimated the mutation probability under the no-delay model using the maximum likelihood method [50] (the same as used by Lee et al.) implemented in the package flan [80]. This procedure correctly reproduced the mutation probability for data from simulations without delay ($n = 0$; SI Fig. S6). For the model with delay, the maximum likelihood fit returned a mutation probability that was lower than the true one (figure 5a); the discrepancy increased with the phenotypic delay. To obtain an apparent mutation probability that is underestimated by a factor of 9.5, as observed by Lee et al. [51], we require $n \approx 30$; i.e. roughly 30 sensitive 'units' of the antibiotic target must be diluted out before a cell becomes phenotypically resistant. Thus, while our simulations do not prove that phenotypic delay is responsible for the discrepancy observed by Lee et al., they suggest that it is a plausible explanation.

2.5 Mutant number distributions may support the existence of phenotypic delay

Our results suggest that a phenotypic delay caused by dilution produces a characteristic (though small) change in the shape of the observed mutant number distribution (figure 4b). This deviation should be in principle detectable in experiments. To check this, we used the dataset of Boe et al. [52] for a 1104-replicate fluctuation test, the bacterium *E. coli* and the fluoroquinolone antibiotic nalidixic acid as the selective agent. As explained in Sec. 2.2, we expect that a small number of wild-type DNA gyrases should be enough for the cell to be sensitive, suggesting that phenotypic delay via gyrase dilution may be likely. Boe et al. [52] report an unsatisfactory fit of their mutant number distribution data to the theoretical predictions of two different variants of the Luria-Delbrück model (the Lea-Coulson and Haldane models); in comparison to theory, Boe et al. observed too many experiments yielding either no mutants or a high number of mutants (greater than 16), and a dearth of experiments resulting in intermediate mutant counts (1-16). Qualitatively, this seems to be consistent with our expectations for the dilution model (figure 4a).

To see if the dilution model of phenotypic delay indeed provides a superior fit to Boe et al's data, we used an approximate Bayesian computation (ABC) approach [81] (Methods). We simulated a 1104-replicate fluctuation experiment 10^4 times, for both the model with and without delay, with initial and final population sizes of 1.2×10^4 and 1.2×10^9 matching those of Boe et al. [52]. We then determined the posterior Bayesian probability that the experimental data is generated by the
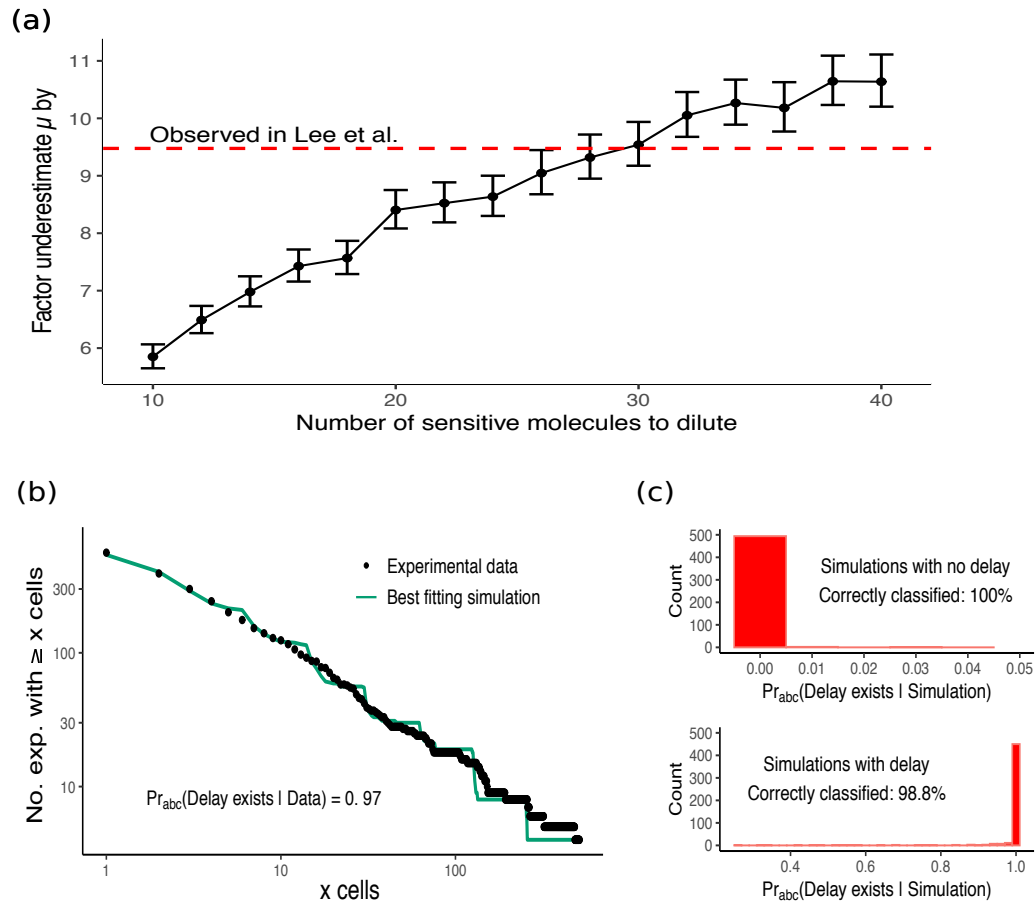
Figure 5: **Phenotypic delay due to the dilution mechanism explains observed discrepancy in mutation rates and provides superior fit to fluctuation experiment data**. (a) We simulated the fluctuation experiment of Ref. [51], where the authors report a factor of 9.5 difference between μ obtained by DNA sequencing and fluctuation tests. For each n we simulated 1000 experiments with the sequencing-derived mutation probability $\mu = 3.98 \times 10^{-9}$ and then used the same estimation procedure as Ref. [51] to infer μ assuming no delay exists. $n = 30$ sensitive molecules are required to account for the discrepancy observed. Error bars are $1.96 \times$ standard error. (b) The experimental cumulative mutant frequency distribution reported by Boe et al. [52] (black points) and the best-fit simulated distribution (green line) for the dilution phenotypic delay model. (c) Histograms of the probability of the delay model obtained by applying the approximate Bayesian computation scheme to simulated data. Our classification algorithm correctly discriminates between the models.

delay model as opposed to the no-delay model. We also examined the validity of our approach on synthetic data, see figure 5c and Methods and models for details. We obtain that the probability of the experimental data coming from the model with phenotypic delay is 0.97. We thus conclude that the Boe et al. data supports the existence of phenotypic delay caused by the dilution mechanism.

3   Discussion

Quantitative models for *de novo* evolution of drug resistance are an important tool in tackling bacterial antimicrobial resistance, as well as viral infections and cancer. However, our quantitative understanding of how resistance emerges is still limited. The possibility of a phenotypic delay between the occurrence of a genetic mutation and its phenotypic expression has long been discussed [29, 30, 31, 32, 33], but its relevance for bacteria evolution has been questioned until recently [35]. Here, we have used computer simulations and theory to study the effects of phenotypic delay on the emergence of bacterial resistance to antibiotics. We investigated three different mechanisms that could lead to phenotypic delay: (i) dilution of antibiotic-sensitive molecules, (ii) effective polyploidy, and (iii) accumulation of resistance-enhancing molecules. We observe that the third mechanism only leads to phenotypic delay under a limited range of parameters, which makes it unlikely to be biologically relevant. The other two mechanisms have different "control parameters" (the degree of ploidy c versus the number of target molecules n) and different effects on the population dynamics. In particular, we show that protein dilution, but not effective polyploidy, can affect the probability that a growing population survives antibiotic treatment. The same mechanism is responsible for biasing the estimated mutation rate in a Luria-Delbrück fluctuation test. Effective polyploidy does not play a role here because of two cancelling effects: increased ploidy increases the number of mutations per cell in the growing population, but also increases the length of the phenotypic delay. These effects counterbalance such that the Luria-Delbrück distribution remains unaffected [35].

Effect of the dilution mechanism on fluctuation test data. Luria-Delbrück fluctuation tests are the standard microbiological method still being used for estimating mutation rates, yet it has often been noted that the measured distributions of mutant numbers do not quite fit the theoretical distribution [33, 30, 34, 52]. A comparison with a more direct approach (DNA sequencing) suggests that fluctuation tests can significantly underestimate mutation rates [51]. Although phenotypic delay has been suggested as a possible explanation for these effects [33, 51], our study is the first to investigate in detail how specific mechanisms of phenotypic delay alter the shape of the Luria-Delbrück distribution, and to demonstrate that it can indeed produce a biased mutation rate estimate of the same order of magnitude as that observed experimentally [51]. We also show that the simulated distribution from the dilution model fits the experimental fluctuation test data of Boe et al.[52] better than the standard model without phenotypic delay. We note that this result should however be taken cautiously. Boe et al.'s experimental protocol is not ideal for detecting phenotypic delay: for example, their bacterial cultures were allowed to reach stationary phase before plating. Moreover, our work shows that while phenotypic delay due to dilution affects the mutant number distribution, the change is subtle, requiring many replicate experiments to produce statistically significant results. While the usual number of replicates in a fluctuation test is less than 100, recent developments in automated culture methods should make it possible to run fluctuation tests with many more replicates, which may provide a way to probe the effects of phenotypic delay on the Luria-Delbrück distribution in more detail.

From molecular detail to evolutionary population dynamics. Our work presents an example of how molecular details at the intracellular level (here, protein dilution and the details of DNA replication) can have a direct effect on evolution at the population level [82, 83, 84]. This observation complements other works showing that, for example, molecular processes such as transcription and translation affect population-level distributions of protein numbers [85, 86] and that noise in gene expression can directly affect the survival of populations in a fluctuating environment [87].

Importantly, both the effective polyploidy mechanism and the dilution mechanism cause a phenotypic delay only if the resistance mutation is *recessive*. For effective polyploidy this implies that a cell must contain only resistant alleles in order to be phenotypically resistant, while for the dilution mechanism we have assumed that sensitive target molecules need to be diluted out (or

otherwise removed). This implies that we would expect to see phenotypic delay in the evolution of resistance to some antibiotics, but not to others. In particular, we would expect phenotypic delay due to dilution if the antibiotic acts by binding to its molecular target to make a toxic adduct, and resistance involves production of a resistant target. This is the case for fluoroquinolone antibiotics, which bind to DNA gyrase, causing DNA double-strand breaks; resistance is caused by production of mutant gyrase that no longer binds the antibiotic [88]. The fact that both Boe et al. [52] and Lee et al. [51] observed discrepancies in fluctuation test data for resistance to the fluoroquinolone nalidixic acid, is consistent with this expectation.

Assumptions of the model. Our simulations and theoretical calculations have involved a number of simplifying assumptions. Firstly, we ignore any possible fitness costs of mutations, assuming equal growth rates for wild-type and mutant cells in the absence of the antibiotic. While many resistance mutations incur a fitness costs [89, 90], many clinically-relevant mutations have either no cost or even a small growth advantage [90, 91].

For the molecular dilution mechanism, we have assumed that the degradation rate of target molecules is negligible, so that sensitive molecules can only be removed through cell division and dilution. While this seems to be (mostly) the case for bacterial enzymes targeted by antibiotics [92, 93], it does not have to be the case for mammalian cells in which degradation plays a bigger role than dilution [94].

We have also assumed that in the dilution mechanism, *all* sensitive molecules need to be removed for the cell to become phenotypically resistant. In reality, resistance is likely to gradually increase as the number of sensitive molecules decreases. Our general conclusions remain valid in this case, however the mutant distribution may change. To construct more accurate models, we need measurements of the degree of antibiotic sensitivity as a function of the intracellular numbers of resistant and sensitive antibiotic targets. While technically challenging, such measurements could be carried out e.g. by fluorescently labelling target molecules [62].

Experimental tests for phenotypic delay Our work suggests that, at least in principle, the mutant number distribution could be used to detect the existence of a phenotypic delay caused by molecular dilution, although this would require many replicate experiments. Sun et al. have demonstrated phenotypic delay due to effective polyploidy more directly by tracking expression of a genetically engineered fluorescent marker in bacterial lineages [35]. Another approach would be an experiment similar to that from figure 1, in which a mutagen such as UV irradiation creates a burst of mutants. Other signatures of phenotypic delay may be detected in experiments where the timing of antibiotic exposure, and of resistance evolution, can be precisely controlled in turbidostat-like continuous culture devices [95].

Broader significance of phenotypic delay We have shown here that phenotypic delay (caused by molecular dilution) can affect mutation rate estimates from fluctuation tests, as well as the probability that a bacterial infection survives antibiotic treatment. Phenotypic delay may also affect other processes. For example, it was recently shown that a delay in evolutionary adaptation can lead to coexistence of spatial populations, in cases where immediate adaptation would eradicate coexistence [96, 97]. In another example, it was suggested that in order to explain the effect of antibiotic pulses of different lengths on the probability of emergence of antibiotic resistance, a delay in evolutionary adaptation (called *physiological memory* by the authors) must be taken into account [98].

4 Methods and models

In all our simulations we use an agent-based model to simulate how mutated cells gain phenotypic resistance. Each cell has a number of attributes depending on the studied mechanism, such as the numbers of sensitive and mutated DNA copies, and the numbers of sensitive and resistant proteins, as specified below. Cells divide after time t_d since last division.

For the population-level simulations (section 2.1), we simulate 100 cells which have just become genotypically resistant. Population-level simulations are repeated 1,000 times and single-cell simulations are repeated 10,000 times.

4.1 Modelling effective polyploidy

To describe how the copy number (ploidy) c changes during cell growth and division we use the Cooper-Helmstetter model [37]. We assume that it takes $t_1 = 40\,\text{min}$ for a DNA replication fork to travel from the origin of replication to the replication terminus, and that the cell divides $t_2 = 20\,\text{min}$ after DNA replication terminated ($t_1 = $ C and $t_2 = $ D in the original nomenclature of Ref. [37]; values representative for *Escherichia coli* strain B/r). During balanced ("steady state") growth assumed in this work, the number of chromosomes must double during the time t_d between cell divisions (population doubling time). This means that for any $t_d < t_1 + t_2 = 60\text{min}$, the cell must have multiple replication forks and more than one copy of the chromosome. The number of chromosomes will fluctuate during cell growth: it will double some time before the division, and decrease by a half just after the division. If t_{ini} is the time since last division at which new replication forks are initiated, we must have $(t_{\text{ini}} + t_1) \mod t_d = t_d - t_2$. This equation states that the time when a replication round initiated in the parent cell finishes in the offspring cell $((t_{\text{ini}} + t_1) \mod t_d)$ must be the same as the time $t_d - t_2$ when the cell division process (lasting t_2 min) is initiated. It can be shown that this gives $t_{\text{ini}} = t_d - (t_1 + t_2) \mod t_d$. We proceed in a similar way to determine the time t_{rep} at which a gene which confers resistance is replicated. If the gene is located in the middle of the genome, as is the case for the gyrA gene relevant for fluoroquinolone resistance, it will be copied $t_1/2$ minutes after chromosome replication initiation. This implies that

$$t_{\text{rep}} = t_d - \left(\left(t_2 + \frac{t_1}{2} \right) \mod t_d \right). \tag{2}$$

At this time point during the cell cycle the copy number of the gene of interest will double. The effective polyploidy immediately after this event is maximal and equal to

$$c = 2^{\lceil \frac{t_1/2 + t_2}{t_d} \rceil}, \tag{3}$$

where $\lceil \dots \rceil$ denotes the ceiling function. We use c from Eq. (3) as the control variable in simulations of the polyploidy model.

To simulate a cell or a population of cells with effective polyploidy we use the following algorithm. We initialize the simulation with all cells having $c/2$ sensitive alleles. Cells replicate in discrete generations every t_d minutes. The number of allele copies double at t_{rep} (Eq. (2)) since the last division in such a way that a sensitive/resistant allele gives rise to a sensitive/resistant copy, respectively. Sensitive alleles have a probability μ of mutating to a resistant allele. When a cell divides, the copies are split between the two daughter cells, with those linked by the most recent replication fork ending up in the same cell. We assume that the resistant mutation is recessive, which implies that a cell becomes resistant when all of its gene copies are resistant.

4.2 Modelling the dilution of sensitive molecules

For the dilution mechanism, we track the number of sensitive target molecules in each cell. We assume that at time zero, all cells have n sensitive target molecules and no resistant ones. When a mutation happens, the mutated cell begins to produce resistant target molecules and ceases to produce new sensitive molecules. At cell division, the sensitive molecules are partitioned between the two daughter cells following a binomial distribution with probability 0.5. We consider that a cell becomes phenotypically resistant when it contains no sensitive molecules. In the supplementary information we relax this assumption and study the case where a cell is considered resistant when the number of sensitive molecules falls below a (non-zero) threshold value (SI figure S5).

4.3 Modelling the accumulation of resistance-enhancing molecules

To model the accumulation of resistance-enhancing molecules, we explicitly simulate the production of M_p resistance-enhancing molecules per cell cycle and their stochastic division between daughter cells, via a binomial distribution, at cell division. A cell is considered resistant when it contains more than M_r resistance-enhancing molecules. In all simulations we fix $M_r = 1000$ and vary M_p to explore a range of $m = \frac{M_p}{M_r}$ between 0.5 and 2.

4.4 Combining effective polyploidy and molecular dilution

To include both effective polyploidy and molecular dilution, we track explicitly the total gene copies, the resistant gene copies and the number of sensitive proteins, as explained in Secs. 4.1 and 4.2. We assume that the number of resistant proteins produced in one cell cycle is proportional to the ratio of resistant to total gene copies. Both types of proteins (sensitive and resistant) are partitioned at cell division following a binomial distribution with probability 0.5. We consider that a cell becomes phenotypically resistant when it contains no sensitive molecules.

4.5 Simulating a growing infection

We start our simulations with 100 sensitive bacteria. Bacteria reproduce in discrete generations with doubling time t_d. Upon reproduction, each bacterium can mutate with probability $\mu = 10^{-7}$. When the population reaches 10^7 cells, all phenotypically sensitive cells are removed (killed); this represent antimicrobial therapy. We repeat the simulation 1000 times to obtain the survival probability as a fraction of simulations in which phenotypically resistant cells emerge before the population dies out.

4.6 Simulating Luria-Delbrück fluctuation tests

To generate mutant size distributions for realistically large population sizes of sensitive cells required for comparing the model with experimental data, we use an algorithm based on the Çinlar's method [99, 100]. The algorithm does not simulate the sensitive population explicitly, but it generates a set of times $\{t_i\}$ at which mutants emerge from the exponentially growing sensitive population (formally, t_i is the time generated from a Poisson process with probability $\mu\lambda_s e^{\lambda_s(1-\mu)t_i}$):

Algorithm 1:

---
1 Initialize $t = 0$, $s = 0$ $t_i = []$;
2 **while** $t \leq t_f$ **do**
3 $\quad\quad s \leftarrow s - \log(U(0,1))$;
4 $\quad\quad t \leftarrow \frac{1}{\lambda_s} \log\left(\frac{1-\mu}{\mu N_i} s + 1\right)$;
5 $\quad\quad t_i.\text{extend}(t)$
6 **end**
7 return t_i

Here $t_f = \frac{\ln(N_f/N_i)}{\lambda_s}$ is the final time, N_f is the final population size, N_i is the initial population size, $\lambda_s = \frac{\ln(2)}{t_d}(1-\mu)$ is the growth rate of the sensitive bacteria, t_d is the doubling time, μ is the mutation probability and $U(0,1)$ is a random variable uniformly distributed between 0 and 1.

For each t_i, we then calculate the number of generations until the final time t_f as

$$g_i = \frac{t_f - t_i}{t_d}. \tag{4}$$

For all of the simulations in sections 2.4 and 2.5, we assume $t_d = 60\,\text{min}$. We then simulate each clone for g_i generations, including dilution of sensitive target molecules, and measure the number of resistant cells for each clone. Finally, we measure the number of resistant cells for each replicate by summing up over all clones.

4.7 Approximate Bayesian computation

We use an approximate Bayesian computation method to determine posterior probabilities of the non-delay and the dilution model. Briefly, the method relies on generating many (here: 10^4) independent samples of the simulated experiment mimicking Boe et al. [52] for both models. Model parameters are sampled from suitable prior distributions, we then select samples that approximate well the real data, and calculate the fraction of best-fit samples corresponding to each model.

A single sample corresponds to 1104 simulated replicates of the fluctuation experiment at fixed parameters, for a given model. For each sample, parameters are randomly chosen from the

15

following prior distributions: $\log_{10}(\mu)$ uniform on $[-10, -8]$, and $\log_2(n)$ uniform on $[0, 8]$ (for the delay model). The tail cumulative mutation function[1]

$$F(k) = \text{Number of experiments yielding} \geq k \text{ mutants}, \quad 0 \leq k \leq 513, \qquad (5)$$

is calculated for each sample i (F_i), and also for the experimental data from Boe et al. [52] (F_{obs}). We then select 100 out of the 2×10^4 (10^4 from each model) generated samples with the smallest Euclidean distance $||F_i - F_{obs}||_2$ (simulated distributions closest to the experimental data). The proportion of these which come from the phenotypic delay model is an approximation of the posterior probability that the experimental data was generated by the delay model (under the assumption that the experimental data was generated by one of the models). In reality the data generation process is likely to be far more complex than our idealised models, but the posterior probability of 0.97 implies the delay model provides a superior explanation to the model with no delay.

To examine the validity of our approach, we performed cross validation. For each model we randomly chose one sample corresponding to that model. We then computed the probability the simulated data was generated by the model with phenotypic delay, via the approximate method detailed above. This was carried out 500 times for each model. The proportion of simulations that were misclassified (as being with delay when they were not, or vice versa) was low (0.006, figure 5c), showing that our model selection framework is able to discriminate between the two models. We provide a further sensitivity analysis of this inference method in Section 7 of the SI.

Acknowledgements

References

[1] C. Holohan, S. Van Schaeybroeck, D. B. Longley, and P. G. Johnston, "Cancer drug resistance: an evolving paradigm," *Nat. Rev. Cancer*, vol. 13, pp. 714–726, 09 2013.

[2] A. L. Hill, D. I. S. Rosenbloom, M. A. Nowak, and R. F. Siliciano, "Insight into treatment of hiv infection from viral dynamics models," *Immunol. Rev.*, vol. 285, no. 1, pp. 9–25, 2018.

[3] E. D. Brown and G. D. Wright, "Antibacterial drug discovery in the resistance era," *Nature*, vol. 529, pp. 336–343, 01 2016.

[4] D. Hughes and D. I. Andersson, "Evolutionary trajectories to antibiotic resistance," *Annu. Rev. Microbiol.*, vol. 71, no. 1, pp. 579–596, 2017.

[5] T. D. Lieberman, K. B. Flett, I. Yelin, T. R. Martin, A. J. McAdam, G. P. Priebe, and R. Kishony, "Genetic variation of a bacterial pathogen within individuals with cystic fibrosis provides a record of selective pressures," *Nature Genetics*, vol. 46, pp. 82–87, 12 2013.

[6] S. J. van Hal, J. A. Steen, B. A. Espedido, S. M. Grimmond, M. A. Cooper, M. T. G. Holden, S. D. Bentley, I. B. Gosbell, and S. O. Jensen, "In vivo evolution of antimicrobial resistance in a series of staphylococcus aureus patient isolates: the entire picture or a cautionary tale?," *J. Antimicrob. Chemother.*, vol. 69, no. 2, pp. 363–367, 2014.

[7] M. M. Mwangi, S. W. Wu, Y. Zhou, K. Sieradzki, H. de Lencastre, P. Richardson, D. Bruce, E. Rubin, E. Myers, E. D. Siggia, and A. Tomasz, "Tracking the in vivo evolution of multidrug resistance in staphylococcus aureus by whole-genome sequencing," *Proc. Natl. Acad. Sci. U.S.A.*, vol. 104, no. 22, pp. 9451–9456, 2007.

---

[1]F is undefined for $k \geq 514$ as the authors of [52] grouped replicates yielding more than 512 mutants.

[8] T. D. Lieberman, J.-B. Michel, M. Aingaran, G. Potter-Bynoe, D. Roux, M. R. Davis Jr, D. Skurnik, N. Leiby, J. J. LiPuma, J. B. Goldberg, A. J. McAdam, G. P. Priebe, and R. Kishony, "Parallel bacterial evolution within multiple patients identifies candidate pathogenicity genes," *Nat. Genet.*, vol. 43, pp. 1275–1280, 11 2011.

[9] A. Wong and R. Kassen, "Parallel evolution and local differentiation in quinolone resistance in pseudomonas aeruginosa," *Microbiology*, vol. 157, no. 4, pp. 937–944, 2011.

[10] E. E. Smith, D. G. Buckley, Z. Wu, C. Saenphimmachak, L. R. Hoffman, D. A. D'Argenio, S. I. Miller, B. W. Ramsey, D. P. Speert, S. M. Moskowitz, J. L. Burns, R. Kaul, and M. V. Olson, "Genetic adaptation by pseudomonas aeruginosa to the airways of cystic fibrosis patients," *Proc. Natl. Acad. Sci. U.S.A.*, vol. 103, no. 22, pp. 8487–8492, 2006.

[11] J. Zdziarski, E. Brzuszkiewicz, B. Wullt, H. Liesegang, D. Biran, B. Voigt, J. Grönberg-Hernandez, B. Ragnarsdottir, M. Hecker, E. Z. Ron, R. Daniel, G. Gottschalk, J. Hacker, C. Svanborg, and U. Dobrindt, "Host imprints on bacterial genomes – rapid, divergent evolution in individual patients," *PLOS Pathogens*, vol. 6, p. e1001078, 08 2010.

[12] S. Suerbaum and C. Josenhans, "Helicobacter pylori evolution and phenotypic diversification in a changing host," *Nat. Rev. Microbiol.*, vol. 5, pp. 441–452, 06 2007.

[13] L. Kennemann, X. Didelot, T. Aebischer, S. Kuhn, B. Drescher, M. Droege, R. Reinhardt, P. Correa, T. F. Meyer, C. Josenhans, D. Falush, and S. Suerbaum, "Helicobacter pylori genome evolution during human infection," *Proc. Natl. Acad. Sci. U.S.A.*, vol. 108, no. 12, pp. 5033–5038, 2011.

[14] Q. Zhang, G. Lambert, D. Liao, H. Kim, K. Robin, C.-k. Tung, N. Pourmand, and R. H. Austin, "Acceleration of emergence of bacterial antibiotic resistance in connected microenvironments," *Science*, vol. 333, no. 6050, pp. 1764–1767, 2011.

[15] E. Toprak, A. Veres, J.-B. Michel, R. Chait, D. L. Hartl, and R. Kishony, "Evolutionary paths to antibiotic resistance under dynamically sustained drug selection," *Nat. Genet.*, vol. 44, pp. 101–105, 12 2011.

[16] M. L. M. Salverda, E. Dellus, F. A. Gorter, A. J. M. Debets, J. van der Oost, R. F. Hoekstra, D. S. Tawfik, and J. A. G. M. de Visser, "Initial mutations direct alternative pathways of protein evolution," *PLoS Genet.*, vol. 7, pp. 1–11, 03 2011.

[17] J. A. G. M. de Visser and J. Krug, "Empirical fitness landscapes and the predictability of evolution," *Nat. Rev. Genet.*, vol. 15, pp. 480–490, 06 2014.

[18] R. C. MacLean, A. R. Hall, G. G. Perron, and A. Buckling, "The population genetics of antibiotic resistance: integrating molecular mechanisms and treatment contexts," *Nat. Rev. Genet.*, vol. 11, pp. 405–414, 2010.

[19] M. Lukačišinová and T. Bollenbach, "Toward a quantitative understanding of antibiotic resistance evolution," *Curr. Opin. Biotechnol.*, vol. 46, pp. 90–97, 2017.

[20] R. Allen and B. Waclaw, "Antibiotic resistance: a physicist's view," *Phys. Biol.*, vol. 13, no. 4, p. 045001, 2016.

[21] B. Waclaw, I. Bozic, M. E. Pittman, R. H. Hruban, B. Vogelstein, and M. A. Nowak, "A spatial model predicts that dispersal and cell turnover limit intratumour heterogeneity," *Nature*, vol. 525, pp. 261–264, 08 2015.

[22] M. D. Nicholson and T. Antal, "Competing evolutionary paths in growing populations with applications to multidrug resistance," *PLOS Computational Biology*, vol. 15, pp. 1–25, 04 2019.

[23] M. A. Nowak, *Evolutionary Dynamics*. Cambridge, Massachusetts: Harvard University Press, 2006.

[24] R. A. Blythe and A. J. McKane, "Stochastic models of evolution in genetics, ecology and linguistics," *J. Stat. Mech.: Theory Exp.*, vol. 2007, no. 07, p. P07018, 2007.

[25] P. M. Altrock, L. L. Liu, and F. Michor, "The mathematics of cancer: integrating quantitative models," *Nat. Rev. Cancer*, vol. 15, pp. 730–745, 2015.

[26] M. M. Desai, D. S. Fisher, and A. W. Murray, "The speed of evolution and maintenance of variation in asexual populations," *Curr. Biol.*, vol. 17, no. 5, pp. 385–394, 2007.

[27] I. Cvijović, B. H. Good, E. R. Jerison, and M. M. Desai, "Fate of a mutation in a fluctuating environment," *Proc. Natl. Acad. Sci. U.S.A.*, vol. 112, no. 36, pp. E5021–E5028, 2015.

[28] T. Paixão, G. Badkobeh, N. Barton, D. Çörüş, D.-C. Dang, T. Friedrich, P. K. Lehre, D. Sudholt, A. M. Sutton, and B. Trubenová, "Toward a unifying framework for evolutionary processes," *J. Theor. Biol.*, vol. 383, pp. 28–43, 2015.

[29] T. M. Sonneborn and R. S. Lynch, "Hybridization and segregation in paramecium aurelia," *J. Exp. Zool.*, vol. 67, no. 1, pp. 1–72, 1934.

[30] P. Armitage, "The statistical theory of bacterial populations subject to mutation," *J. Royal Stat. Soc.*, vol. 14, no. 1, pp. 1–40, 1952.

[31] H. B. Newcombe, "Delayed phenotypic expression of spontaneous mutations in escherichia coli," *Genetics*, vol. 33, no. 5, pp. 447–476, 1948.

[32] B. D. Davis, "The isolation of biochemically deficient mutants of bacteria by means of penicillin," *Proc. Natl. Acad. Sci. U.S.A.*, vol. 35, pp. 1–10, 1949.

[33] S. E. Luria and M. Delbrück, "Mutations of bacteria from virus sensitivity to virus resistance," *Genetics*, vol. 28, no. 6, pp. 491–511, 1943.

[34] F. J. Ryan, "Phenotypic (phenomic) lag in bacteria," *Am. Nat.*, vol. 89, no. 846, pp. 159–162, 1955.

[35] L. Sun, H. K. Alexander, B. Bogos, D. J. Kiviet, M. Ackermann, and S. Bonhoeffer, "Effective polyploidy causes phenotypic delay and influences bacterial evolvability," *PLoS Biol.*, vol. 16, p. 2004644, 02 2018.

[36] P. L. Foster, "Methods for determining spontaneous mutation rates," *Methods Enzymol.*, vol. 409, pp. 195–213, 2006.

[37] S. Cooper and C. E. Helmstetter, "Chromosome replication and the division cycle of escherichia coli b/r," *J. Mol. Biol.*, vol. 31, no. 3, pp. 519–540, 1968.

[38] H. J. Nielsen, B. Youngren, F. G. Hansen, and S. Austin, "Dynamics of *Escherichia coli* chromosome segregation during multifork replication," *J. Bacteriol.*, vol. 189, no. 23, pp. 8660–8666, 2007.

[39] J. D. Wang and P. A. Levin, "Metabolism, cell growth and the bacterial cell cycle," *Nat. Rev. Microbiol.*, vol. 7, pp. 822–827, 2009.

[40] L. L. Silver and K. A. Bostian, "Discovery and development of new antibiotics: the problem of antibiotic resistance.," *Antimicrob. Agents Chemother.*, vol. 37, no. 3, pp. 377–383, 1993.

[41] D. I. Andersson and D. Hughes, "Persistence of antibiotic resistance in bacterial populations," *FEMS Microbiol. Rev.*, vol. 35, no. 5, pp. 901–911, 2011.

[42] K. J. Aldred, R. J. Kerns, and N. Osheroff, "Mechanism of quinolone action and resistance," *Biochemistry*, vol. 53, no. 10, pp. 1565–1574, 2014.

[43] H. I. M., K. Ilkka, and V. Martti, "Increased substitution of phosphate groups in lipopolysaccharides and lipid a of the polymyxin-resistant pmra mutants of salmonella typhimurium: a 31p-nmr study," *Mol. Microbiol.*, vol. 11, no. 3, pp. 481–487, 1994.

18

[44] A. Beceiro, E. Llobet, J. Aranda, J. A. Bengoechea, M. Doumith, M. Hornsey, H. Dhanji, H. Chart, G. Bou, D. M. Livermore, and N. Woodford, "Phosphoethanolamine modification of lipid a in colistin-resistant variants of acinetobacter baumannii mediated by the pmrab two-component regulatory system," *Antimicrob. Agents Chemother.*, vol. 55, no. 7, pp. 3370–3379, 2011.

[45] M. A. Webber and L. J. V. Piddock, "The importance of efflux pumps in bacterial antibiotic resistance," *J. Antimicrob. Chemother.*, vol. 51, no. 1, pp. 9–11, 2003.

[46] R. A. Bonomo, "β-lactamases: A focus on current challenges," *Cold Spring Harbor Perspect. Med.*, vol. 7, no. 1, p. a025239, 2017.

[47] D. M. Livermore, "β-lactamases: quantity and resistance," *Clin. Microbiol. Infect.*, vol. 3, pp. 4S10–4S19, 1997.

[48] B. S. Speer, N. B. Shoemaker, and A. A. Salyers, "Bacterial resistance to tetracycline: mechanisms, transfer, and clinical significance.," *Clinical Microbiology Reviews*, vol. 5, pp. 387–399, Oct. 1992.

[49] P. Greulich, M. Scott, M. R. Evans, and R. J. Allen, "Growth-dependent bacterial susceptibility to ribosome-targeting antibiotics," *Molecular Systems Biology*, 2015.

[50] W. A. Rosche and P. L. Foster, "Determining mutation rates in bacterial populations," *Methods*, vol. 20, pp. 4–17, 2000.

[51] H. Lee, E. Popodi, H. Tang, and P. L. Foster, "Rate and molecular spectrum of spontaneous mutations in the bacterium escherichia coli as determined by whole-genome sequencing," *Proc. Natl. Acad. Sci. U.S.A.*, vol. 109, no. 41, pp. E2774–E2783, 2012.

[52] L. Boe, T. Tolker-Nielsen, K. M. Eegholm, H. Spliid, and A. Vrang, "Fluctuation analysis of mutations to nalidixic acid resistance in escherichia coli.," *J. Bacteriol.*, vol. 176, no. 10, pp. 2781–2787, 1994.

[53] H. Ikehata and T. Ono, "The mechanisms of uv mutagenesis," *J. Radiat. Res.*, vol. 52, no. 2, pp. 115–125, 2011.

[54] A. Shibai, Y. Takahashi, Y. Ishizawa, D. Motooka, S. Nakamura, B.-W. Ying, and S. Tsuru, "Mutation accumulation under uv radiation in escherichia coli," *Sci. Rep.*, vol. 7, no. 1, p. 14531, 2017.

[55] H. Bates, S. K. Randall, C. Rayssiguier, B. A. Bridges, M. F. Goodman, and M. Radman, "Spontaneous and uv-induced mutations in escherichia coli k-12 strains with altered or absent dna polymerase i.," *J. Bacteriol.*, vol. 171, no. 5, pp. 2480–2484, 1989.

[56] G. Kai and A. S. Weber, "Streptomycin-resistant mutant production in a continuous-flow uv mutation device," *J. Ind. Microbiol.*, vol. 8, pp. 107–112, Sep 1991.

[57] C. Kleanthous, P. Rassam, and C. G. Baumann, "Protein–protein interactions and the spatiotemporal dynamics of bacterial outer membrane proteins," *Curr. Opin. Struct. Biol.*, vol. 35, pp. 109–115, 2015.

[58] P. Rassam, N. A. Copeland, O. Birkholz, C. Tóth, M. Chavent, A. L. Duncan, S. J. Cross, N. G. Housden, R. Kaminska, U. Seger, D. M. Quinn, T. J. Garrod, M. S. P. Sansom, J. Piehler, C. G. Baumann, and C. Kleanthous, "Supramolecular assemblies underpin turnover of outer membrane proteins in bacteria," *Nature*, vol. 523, pp. 333–336, 06 2015.

[59] M. A. de Pedro, C. G. Grünfelder, and H. Schwarz, "Restricted mobility of cell surface proteins in the polar regions of escherichia coli," *J. Bacteriol.*, vol. 186, no. 9, pp. 2594–2602, 2004.

[60] T. Bergmiller, A. M. C. Andersson, K. Tomasek, E. Balleza, D. J. Kiviet, R. Hauschild, G. Tkačik, and C. C. Guet, "Biased partitioning of the multidrug efflux pump acrab-tolc underlies long-lived phenotypic heterogeneity," *Science*, vol. 356, no. 6335, pp. 311–315, 2017.

[61] S. Chong, C. Chen, H. Ge, and X. S. Xie, "Mechanism of transcriptional bursting in bacteria," *Cell*, vol. 158, pp. 314–326, 2014.

[62] M. Stracy, A. J. M. Wollman, E. Kaja, J. Gapinski, J.-E. Lee, V. A. Leek, S. J. McKie, L. A. Mitchenall, A. Maxwell, D. J. Sherratt, M. C. Leake, and P. Zawadzki, "Single-molecule imaging of DNA gyrase activity in living Escherichia coli," *Nucleic Acids Res.*, vol. 47, pp. 210–220, 11 2018.

[63] S. Hui, J. M. Silverman, S. S. Chen, D. W. Erickson, M. Basan, J. Wang, T. Hwa, and J. R. Williamson, "Quantitative proteomic analysis reveals a simple strategy of global resource allocation in bacteria," *Mol. Syst. Biol.*, vol. 11, no. 2, 2015.

[64] M. Schaechter, O. Maaløe, and N. O. Kjeldgaard, "Dependency on medium and temperature of cell size and chemical composition during balanced growth of salmonella typhimurium," *J. Gen. Microbiol.*, vol. 19, no. 3, pp. 592–606, 1958.

[65] O. Pierucci, "Dimensions of escherichia coli at various growth rates: model for envelope growth," *J. Bacteriol.*, vol. 135, no. 2, pp. 559–574, 1978.

[66] S. Vadia and P. A. Levin, "Growth rate and cell size: a re-examination of the growth law," *Curr. Opin. Microbiol.*, vol. 24, pp. 96–103, 2015.

[67] S. Jun, F. Si, R. Pugatch, and M. Scott, "Fundamental principles in bacterial physiology– history, recent progress, and the future with focus on cell size control: a review," *Rep. Prog. Phys.*, vol. 81, no. 5, p. 056601, 2018.

[68] H. K. Alexander, G. Martin, O. Y. Martin, and S. Bonhoeffer, "Evolutionary rescue: linking theory for conservation and medicine," *Evol. Appl.*, vol. 7, no. 10, pp. 1161–1179, 2014.

[69] I. Bozic and M. A. Nowak, "Resisting resistance," *Annual Review of Cancer Biology*, vol. 1, no. 1, pp. 203–221, 2017.

[70] D. E. Lea and C. A. Coulson, "The distribution of the numbers of mutants in bacterial populations," *J. Genet.*, vol. 49, p. 264, Dec 1949.

[71] Q. Zheng, "Progress of a half century in the study of the luria-delbrück distribution," *Math. Biosci.*, vol. 162, no. 1, pp. 1–32, 1999.

[72] S. Sarkar, "Haldane's solution of the luria-delbrück distribution.," *Genetics*, vol. 127, no. 2, pp. 257–261, 1991.

[73] W. T. Ma, G. V. Sandri, and S. Sarkar, "Analysis of the luria-delbrück distribution using discrete convolution powers," *J. Appl. Probab.*, vol. 29, no. 2, pp. 255–267, 1992.

[74] C. M. Holmes, M. Ghafari, A. Abbas, V. Saravanan, and I. Nemenman, "Luria-delbrück, revisited: the classic experiment does not rule out lamarckian evolution," *Phys. Biol.*, vol. 14, no. 5, p. 055004, 2017.

[75] P. Keller and T. Antal, "Mutant number distribution in an exponentially growing population," *J. Stat. Mech.: Theory Exp.*, vol. 2015, no. 1, p. P01011, 2015.

[76] M. D. Nicholson and T. Antal, "Universal asymptotic clone size distribution for general population growth," *Bull. Math. Biol.*, vol. 78, pp. 2243—-2276, 2016.

[77] D. Fusco, M. Gralka, J. Kayser, A. Anderson, and O. Hallatschek, "Excess of mutational jackpot events in expanding populations revealed by spatial luria–delbrück experiments," *Nat. Commun.*, vol. 7, p. 12760, 10 2016.

[78] D. Cheek and T. Antal, "Mutation frequencies in a birth–death branching process," *Ann. Appl. Probab.*, vol. 28, pp. 3922–3947, 12 2018.

[79] F.-A. Fortin, F.-M. De Rainville, M.-A. Gardner, M. Parizeau, and C. Gagné, "DEAP: Evolutionary algorithms made easy," *J. Mach. Learn. Res.*, vol. 13, pp. 2171–2175, 2012.

[80] A. Mazoyer, R. Drouilhet, S. Despréaux, and B. Ycart, "flan: An R Package for Inference on Mutation Models," *The R Journal*, vol. 9, no. 1, pp. 334–351, 2017.

[81] M. A. Beaumont, W. Zhang, and D. J. Balding, "Approximate bayesian computation in population genetics," *Genetics*, vol. 162, no. 4, pp. 2025–2035, 2002.

[82] D. Noble, "Biophysics and systems biology," *Philos. Trans. R. Soc., A*, vol. 368, no. 1914, pp. 1125–1139, 2010.

[83] J. M. Vilar and L. Saiz, "Systems biophysics of gene expression," *Biophys. J.*, vol. 104, no. 12, pp. 2574–2585, 2013.

[84] A. E. Sgro, D. J. Schwab, J. Noorbakhsh, T. Mestler, P. Mehta, and T. Gregor, "From intracellular signaling to population oscillations: bridging size- and time-scales in collective behavior," *Mol. Syst. Biol.*, vol. 11, no. 1, 2015.

[85] N. Brenner, E. Braun, A. Yoney, L. Susman, J. Rotella, and H. Salman, "Single-cell protein dynamics reproduce universal fluctuations in cell populations," *Eur. Phys. J. E: Soft Matter Biol. Phys.*, vol. 38, p. 102, Sep 2015.

[86] N. Brenner, C. M. Newman, D. Osmanović, Y. Rabin, H. Salman, and D. L. Stein, "Universal protein distributions in a model of cell growth and division," *Phys. Rev. E*, vol. 92, p. 042713, Oct 2015.

[87] M. Acar, J. T. Mettetal, and A. van Oudenaarden, "Stochastic switching as a survival strategy in fluctuating environments," *Nat. Genet.*, vol. 40, p. 471, 03 2008.

[88] K. Drlica and X. Zhao, "DNA gyrase, topoisomerase IV, and the 4-quinolones.," *Microbiology and molecular biology reviews*, vol. 61, no. 3, pp. 377–392, 1997.

[89] D. I. Andersson and B. R. Levin, "The biological cost of antibiotic resistance," *Curr. Opin. Microbiol.*, vol. 2, no. 5, pp. 489–493, 1999.

[90] A. H. Melnyk, A. Wong, and R. Kassen, "The fitness costs of antibiotic resistance mutations," *Evol. Appl.*, vol. 8, no. 3, pp. 273–283, 2015.

[91] E. C. Böttger, B. Springer, M. Pletschette, and P. Sander, "Fitness of antibiotic-resistant microorganisms and compensatory mutations," *Nat. Med.*, vol. 4, p. 1343, 12 1998.

[92] K. Nath and A. L. Koch, "Protein degradation in escherichia coli : I. measurement of rapidly and slowly decaying components," *J. Biol. Chem.*, vol. 245, no. 11, pp. 2889–2900, 1970.

[93] M. Hintsche and S. Klumpp, "Dilution and the theoretical description of growth-rate dependent gene expression," *J. Biol. Eng.*, vol. 7, p. 22, Sep 2013.

[94] E. Eden, N. Geva-Zatorsky, I. Issaeva, A. Cohen, E. Dekel, T. Danon, L. Cohen, A. Mayo, and U. Alon, "Proteome half-life dynamics in living human cells," *Science*, vol. 331, no. 6018, pp. 764–768, 2011.

[95] N. Ojkic, E. Lilja, S. Direito, A. Dawson, R. J. Allen, and B. Waclaw, "A roadblock-and-kill model explains the dynamical response to the DNA-targeting antibiotic ciprofloxacin," *bioRxiv*, p. 791145, Oct. 2019.

[96] M. Bauer and E. Frey, "Multiple scales in metapopulations of public goods producers," *Phys. Rev. E*, vol. 97, p. 042307, Apr 2018.

[97] M. Bauer and E. Frey, "Delayed adaptation in stochastic metapopulation models," *Europhys. Lett.*, vol. 122, no. 6, p. 68002, 2018.

[98] W.-H. Lin and E. Kussell, "Complex interplay of physiology and selection in the emergence of antibiotic resistance," *Curr. Biol.*, vol. 26, no. 11, pp. 1486–1493, 2016.

[99] E. Çinlar, *Introduction to Stochastic Processes*. Mineola, New York: Dover Publications, 1975.

[100] R. Pasupathy, "Generating nonhomogenous Poisson processes," in *Wiley Encyclopedia of Operations Research and Management Science*, Wiley, 2011.